COMMUNICATION

Mechanochemical preparation of piezoelectric nanomaterials: BN, MoS_2 and WS_2 2D materials and their glycine-cocrystals

Received 00th January 20xx,
Accepted 00th January 20xx

DOI: 10.1039/x0xx00000x

Viviana Jehová González,[a] Antonio M. Rodríguez,*[a] Ismael Payo,[b] Ester Vázquez*[a,c]

Different 2D-layered materials of transition metal dichalcogenides (TMDCs) such as boron nitride (BN) or molybdenum disulphide (MoS_2) have been theorised to have piezoelectric behaviour. Still, the procedures to obtain these nanomaterials, with the right quality and quantity to observe the piezoelectric performance, are enormously expensive, halting its possible applications. Here, we show the mechanochemical exfoliation of 2D nanomaterials (FLG, BN, MoS_2 and WS_2) with glycine. We have also successfully synthesised the cocrystals for these nanomaterials, which makes it possible to enhance their piezoelectric responses.

Piezoelectric materials have a unique property that converts mechanical energy into electrical energy or viceversa[1]. Barium titanate is the first piezoelectric ceramic ever discovered, but the ceramic lead zirconate titanate, also known as PZT, is the most commonly used material for piezoelectric harvesting.[2] Nevertheless, the extremely fragile nature of PZT ceramic and the incorporation of lead create issues such as the reliability, durability, and safety of this material for long-term sustainable operation.

2D materials and the possibility to modulate their composition in a well-controlled manner offer a platform that allows the creation of different heterostructures for a large variety of applications. Starting with graphene, 2D nanomaterials have grown to include insulator (boron nitride, BN), semiconductors (molybdenum disulphide, MoS_2) and metals (Niobium diselenide, $NbSe_2$).[3] Together with other different properties, the theoretical piezoelectricity of single-atomic layers of boron nitride (BN), molybdenum disulfide (MoS_2) and tungsten disulfide (WS_2) as a function of strain-induced lattice distortion and ionic charge polarisation has been studied.[4, 5] The future perspective of these nanomaterials have been covered in the literature.[6] Experimentally, some applications of this nanomaterial behaviour have been explored in energy conversion,[7] voltage generators,[8] pressure sensors,[9] nonlinear energy harvesters,[10] and transducers.[11] The methodologies currently used in the production of these nanomaterials for the nano-electromechanical applications are mainly based on chemical vapour deposition (CVD). This technique presents some problems, such as the high cost and necessity to deposit on other materials, which can lead to compatibility issues. Additionally, in real-world applications, the environmental impact of producing any device should always be considered beforehand, and one fundamental problem is to scale up experiments in a safe, secure and efficient way. In that sense, mechanochemical exfoliation of 2D materials has gained increasing importance in the last years.[12-15] These protocols have many advantages over their liquid-phase counterparts, including processes with shorter reaction times, higher product yields and the elimination of (harmful) organic solvents, which make the approach more sustainable and cheaper. Some examples have seen molecules such as sucrose, urea and boric acid used as exfoliating agents.[16-18] Nowadays, there are no examples of the application of TMDCs nanomaterials in piezoelectric paint, coatings or adhesive matrices which could be easily applied to heterogeneous surfaces paving the way for applications such as sensors,[19] or power sensors[20] and nanosystems for harvesting energy applications.[21, 22]

On the other hand, in the past 60 years, piezoelectricity has been confirmed in a variety of biological materials, such as fibrous proteins collagen,[23] elastin,[24] bone[25] (calcified collagen), wood,[26] and some viruses[27] exhibit relatively modest piezoelectricity (0.1–10 pm V^{-1}). Classical piezoelectric principles have also been applied to similar uniaxially orientated, bioactive polymers, such as poly (L-lactic acid) (PLLA), poly (γ-benzyl glutamate) (PBG), and cellulose.[28] The only non-chiral amino acid, glycine, has been known to crystallize in three distinct polymorphs (α)-alpha,[29] (β)-beta,[30] and (γ)-gamma glycine[31] under ambient conditions.[32] The

[a] Instituto Regional de Investigación Científica Aplicada (IRICA), UCLM, 13071 Ciudad Real, Spain.
[b] Escuela de Ingeniería Industrial y Aeroespacial de Toledo, UCLM, Avenida Carlos III s/n, Real Fábrica de Armas, 45071, Toledo, Spain.
[c] Facultad de Ciencias y Tecnologías Químicas, UCLM, Avda. Camilo José Cela S/N, 13071, Ciudad Real, Spain.

Electronic Supplementary Information (ESI) available: [details of any supplementary information available should be included here]. See DOI: 10.1039/x0xx00000x

crystallization of α-glycine occurs in the centrosymmetric space group $P2_1/c$, which precludes piezoelectricity. On the other hand, β-glycine and γ-glycine belong to the non-centrosymmetric space groups P21 and P32, respectively, and so should exhibit a non-zero piezoelectric response. A modest 'effective' shear and longitudinal piezoelectricity have been measured for β-glycine (6 pm V^{-1}) and γ-glycine (10 pm V^{-1}), respectively,[33, 34] using piezo response force microscopy (PFM).[35]

In previous work, we have investigated the exfoliation procedures of graphite to graphene using ball milling techniques in the presence of carbohydrates.[36] We could also prepare glucose-graphene cocrystals as biocompatible systems. In this work, we have explored the exfoliation of 2D nanomaterials using the amino acid glycine. In a second step, the formation of glycine-nanomaterials cocrystals has proven to enhance the piezoelectric properties of the exfoliated material. The relative ease of production of these materials through our mechano-chemical process would significantly impact its presence in future applications. In this study, we proposed a mechanochemical exfoliation of TMDCs and other 2D nanomaterials, such as BN and FLG, and the study of its intrinsic piezoelectricity. Furthermore, our objective aims to integrate the ~~TMDCs~~ nanomaterials in supramolecular organic matrices, such as cocrystals that would enhance their piezoelectricity.

Based on our previous experience on mechanochemical exfoliation of graphite, we performed the ball-milling treatment in solvent-free conditions adding glycine as the exfoliant agent and graphite in a 250 mL stainless-steel grinding bowl with 15 stainless steel balls (2 cm diameter each) at a 250 rpm. The detail experimental procedure is collected in the SI. Since, no precipitate was observed in the resulting dispersions, they were entirely lyophilised after the dialysis. The best experimental conditions for obtaining graphene materials of two different sizes and the yields are represented in table S1.

Fig. S1 displays the Raman spectra of FLG1 and FLG2, showing the different characteristic bands present in carbon nanomaterials (D, G and 2D).[37, 38] It is possible to observe the I_D/I_G value between the different peaks in sample FLG1 is 0.39 in comparison with FLG2, 1.63. This data correlates with the minor size of FLG2 flakes (Table S1, Fig. S2) which shows a direct relation with the time of mechanochemical treatment. Thermogravimetrical analysis (TGA) of these materials is collected in Fig. S3. Our analysis showed a minor presence of nitrogen attached on the graphene layer with a minor presence of oxygen and organic groups on the surface of graphene (2% loss in TGA). We can draw similar conclusions regarding the TGA loss for both FLG1 and FLG2 nanomaterials as in our previous works.[36]

Based on these good results, the high-quality exfoliation with very high yields and the smooth, sustainable and low-cost procedure, we decided to extrapolate these experimental procedures to the exfoliation of other 2D-layered materials such as BN, MoS_2 and WS_2. The experimental conditions for the 2D nanomaterial exfoliation are collected in Table S1. Powder X-Ray Diffraction (PXRD) of the exfoliated materials and the raw nanomaterials are all shown in Fig. S4. In all cases, the x-ray diffraction patterns show a clear decrease in the number of counts on the 002-diffraction pattern. For the example of BN, which has the lowest reduction, it is known that intensity ratio of $(BN_{raw})_{002}$/ $(BN_{exfo})_{002}$ of approximately 2.5 already indicates thin BN layers and much weaker stacking at the c-direction in the exfoliated sample.[39, 40]

Fig. S5 shows the Raman spectra of the MoS_2 system, although both WS_2 and MoS_2 have similar patterns. Both nanomaterials possess two primary Raman modes, one in-plane mode of Mo or W-S bond (E_{2g}) another out-of-plane mode (A_{1g}) at around 380 and 405 cm^{-1} (MoS_2), and 350 and 415 cm^{-1} (WS_2).[41] It is possible to observe a blueshift and a redshift in A_{1g} mode for MoS_2 and WS_2 respectively, which corresponds to a decrease in the number of layers (Table S2). According to the diagrams of Terrones *et al.* for WS_2 nanomaterials,[42] we have a relation of I_{E2g}/I_{A1g} of 0.69 which corresponds to a value of 3 layers for our WS_2 exfoliated nanomaterial. With respect to MoS_2,[43] according to the distance between the bands E^1_{2g} and A_{1g}, the average number of layers is around 3. Finally, BN exhibits a characteristic Raman peak for E2g phonon mode (B-N vibration mode) around 1365 cm^{-1},[44] which is analogous to E2g mode (G band) in graphene. Moreover, a slight blue shift in the E2g peak is consistent with the exfoliation of BN.[45] TEM images (Fig. 1) show the exfoliated dichalcogenide with the corresponding distribution of lateral size in table S1. As shown in Fig. S6, the

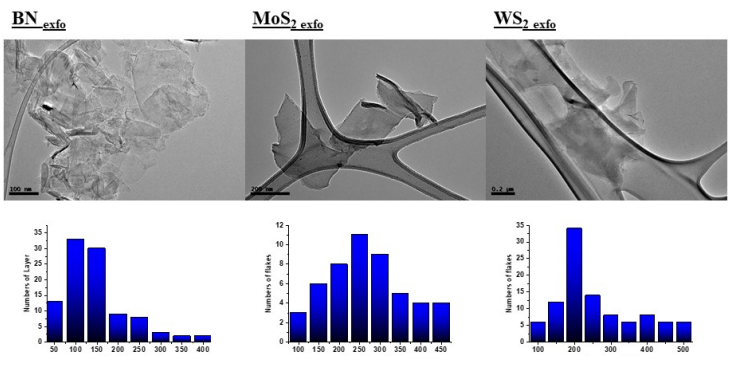

Figure 1. TEM images and distributions of sizes for the different 2D nanomaterials samples.

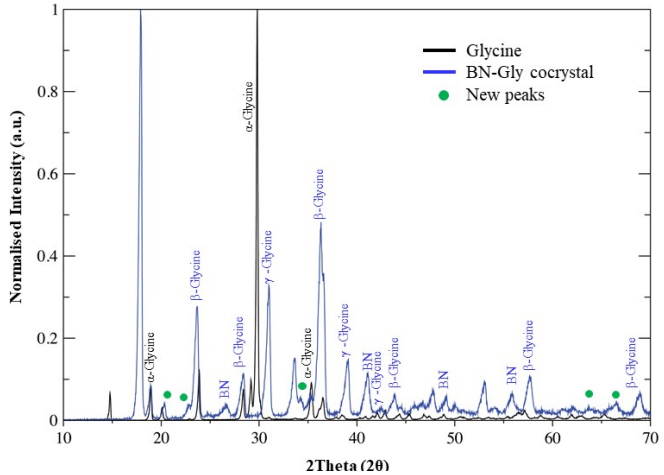

Figure 2. Powder X-ray diffraction results for glycine and BN–glycine cocrystals.

TGA curves of exfoliated nanomaterials show a reduced weight loss compared with those of the pristine 2D nanomaterial because of the small residue of exfoliant agent. Also, a wide scan XPS spectra has been included in the SI to rule out the presence of other impurities (Fig. S7 and Table S3). The atomic content (in %) corresponding to C, N, H and O also correlates with the small quantities of exfoliant agent. Raw and exfoliated materials are not expected to contain C and O. However around 10% of the undesired C and O content probably arises from CO and CO_2 species in air, adsorbed on the substrates.[46] Nevertheless, further analysis of the samples has shown that the sample BN_{exfo} has a residue amount of glycine around 20%, which also corresponds to our TGA analysis (in Fig. S6).

These results are similar to those observed in the literature.[47]

Once demonstrated the exfoliation of 2D nanomaterials, we studied the formation of glycine cocrystals following a similar procedure of lyophilization (SI). The PXRD study for all the different materials indicated that cocrystal structures differed wildly from the original nanomaterials or the initial glycine crystal structure (Fig. 2 for the BN). The appearance of some new peaks (between 20 and 65º) correspond to the different reflections of α, β, and γ-glycine phases in the cocrystal sample and other new peaks in that same region, which do not correspond to any raw material. Those new peaks can be attributed to new cocrystal structures. Similar results are observed for other nanomaterials (Fig. S8). It seems that the presence of the nanomaterial in dispersion together with the crystallization of water while freezing, "pressed out" glycine forcing the appearance of different polymorphisms. This is a process known in the literature,[48, 49] and it correlates well with our understanding on the important interactions between water molecules, exfoliating agents and 2D materials.[50] The TGA for the 2D nanomaterial cocrystals shows a similar loss to glycine, which might be due to the high content of such molecule. The 3wt% of difference between glycine and the cocrystal measurement, corresponds to the presence of the nanomaterial in the cocrystal structure. The structure of glycine cocrystals has been investigated, showing the presence of γ and β-glycine. Commercial glycine was similarly grinded as benchmark sample, resulting in β-glycine majority and with similar piezoelectric response to initial glycine. A comparison of the powder X-ray diffraction results of these samples can be found in Fig. S9. Further study of the Raman spectra of 2D nanomaterial glycine cocrystals pointed to modifications on the vibrational mode frequencies of the intermolecular and intramolecular bonds in the samples. This could correspond to the appearance of new crystal forms and it also gives information on the quality of the exfoliated nanomaterials (Fig. S10).

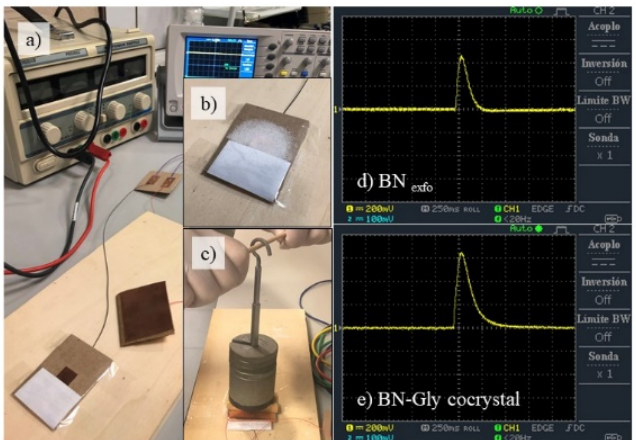

Figure 3. a) Experimental set up for piezoelectricity measurements. b) Layer of cocrystals on a square copper electrode (10 mm × 10 mm), insulated with paper. c). Manual compression of a 2D nanomaterial crystal layer. d) Piezoelectric response of exfoliated BN nanomaterials. e) Measured piezoelectric response with exfoliated BN cocrystals.

Finally, preliminary studies of the piezoelectricity of the exfoliated nanomaterials and the glycine cocrystal forms were performed. Fig. 3 shows the experimental setup used for dynamic testing of the piezoelectricity. Results were amplified with an electronic circuit as shown in Fig. S11. The nanomaterials were placed in a simple system, sandwiched between electrodes of area 1 cm^2, under a force of 10 N. This experimental setup mimics those described in the literature for the experimental corroboration of the piezoelectricity of different materials in powder form.[51]

Table 1. Comparison of piezoelectric response raw and exfoliated 2D nanomaterials and its cocrystals. PZT has been used as a model piezoelectric material.

Sample	Piezoelectric response ($mV \cdot N^{-1}$)
PZT	16
Polyvinylidene fluoride (PVDF)	48
Glycine (Gly)	12
$Gly_{grinded}$	15
$Gly_{lyophilised}$	36
BN_{raw}	8
BN_{exfo}	48
BN- Gly cocrystal	64
BN_{exfo} + Gly-mix	37
$WS_{2\ raw}$	--[a]
$WS_{2\ exfo}$	--[b]
WS_2 - Gly cocrystal	88
$WS_{2\ exfo}$ + Gly-mix	60
Graphite	--[a]
FLG_{exfo}	--[a]
FLG- Gly cocrystal	95
FLG_{exfo} + Gly-mix	60
$MoS_{2\ raw}$	--[b]
$MoS_{2\ exfo}$	--[b]
MoS_2 - Gly cocrystal	150
$MoS_{2\ exfo}$ + Gly-mix	78

[a]These nanomaterials can't be properly measured because its relatively high conductivity, it short-circuited the electronic. [b]Given the semiconductor behaviour of MoS_2, the materials could be working as super-capacitor in the measurement. Attached the figures in the supplementary material (SI).

The piezoelectricity behaviour is better in the cocrystal form than in the exfoliated material or with unpolarized PZT powders (table 1, Fig. S12 and Fig S13) or other organic piezoelectric materials. We obtained similar results for all nanomaterials in their cocrystal form, with a maximum open-circuit voltage of 150 $mV \cdot N^{-1}$ for the MoS_2-$Gly_{cocrystal}$. Similar results could be

observed with the MoS_2 and WS_2 at the same range of induced strain (Table 1). For comparison purposes, we also mixed thoroughly the samples of the exfoliated samples and the glycine cocrystal separately (Table 1 samples: 2D nanomaterial + Gly_{mix}), but it showed less piezoelectric response.

Also, both BN and WS_2 cocrystals showed outstanding responsiveness under lower ranges of forces (around 1N) and produced good recovery cycles and maintained in time (Fig. S14). The remarkable piezoelectric character of these nanomaterials has all been measured without polarisation, while the standard procedure uses polarized materials for this sort of measurements.

Conclusions

We describe an easy and scalable method to enhance the piezoelectric responses of 2D nanomaterials. The process includes the preparation of glycine- 2D cocrystals in which the proportion of different polymorphisms of glycine is readily changed. These powder samples, with different 2D materials, can be used in the development of matrices with piezoelectric character. These materials could be imbedded on paints or inks to cover large surfaces, either in mobile devices, tablets, keyboard, with improved piezoelectric properties. Future uses in sensors, power sensors or in harvesting energy applications can be predicted.

Conflicts of interest

There are no conflicts to declare.

Notes and references

1. K. Uchino, in *Advanced Piezoelectric Materials*, 2017, DOI: 10.1016/b978-0-08-102135-4.00001-1, pp. 1-92.
2. D. Damjanovic, *Reports on Progress in Physics*, 1998, **61**, 1267-1324.
3. A. K. Geim and I. V. Grigorieva, *Nature*, 2013, **499**, 419-425.
4. K. A. N. Duerloo, M. T. Ong and E. J. Reed, *J. Phys. Chem. Lett.*, 2012, **3**, 2871-2876.
5. A. A. M. Noor, H. J. Kim and Y. H. Shin, *Phys. Chem. Chem. Phys.*, 2014, **16**, 6575-6582.
6. M. Samadi, N. Sarikhani, M. Zirak, H. Zhang, H.-L. Zhang and A. Z. Moshfegh, *Nanoscale Horizons*, 2018, **3**, 90-204.
7. W. Wu, L. Wang, Y. Li, F. Zhang, L. Lin, S. Niu, D. Chenet, X. Zhang, Y. Hao, T. F. Heinz, J. Hone and Z. L. Wang, *Nature*, 2014, **514**, 470-474.
8. S. Yu, K. Eshun, H. Zhu and Q. Li, *Sci Rep*, 2015, **5**, 12854.
9. S. Wagner, C. Yim, N. McEvoy, S. Kataria, V. Yokaribas, A. Kuc, S. Pindl, C. P. Fritzen, T. Heine, G. S. Duesberg and M. C. Lemme, *Nano Lett*, 2018, **18**, 3738-3745.
10. M. Lopez-Suarez, M. Pruneda, G. Abadal and R. Rurali, *Nanotechnology*, 2014, **25**, 175401.
11. F. Zhao, Y. Yao, X. Li, L. Lan, C. Jiang and J. Ping, *Anal Chem*, 2018, **90**, 11658-11664.
12. V. León, A. M. Rodríguez, P. Prieto, M. Prato and E. Vazquez, *ACS nano*, 2014, **8**, 563-571.
13. V. Leon, J. M. Gonzalez-Dominguez, J. L. Fierro, M. Prato and E. Vazquez, *Nanoscale*, 2016, **8**, 14548-14555.
14. M. Buzaglo, E. Ruse, I. Levy, R. Nadiv, G. Reuveni, M. Shtein and O. Regev, *Chemistry of Materials*, 2017, **29**, 9998-10006.
15. J. M. Gonzalez-Dominguez, V. Leon, M. I. Lucio, M. Prato and E. Vazquez, *Nat Protoc*, 2018, **13**, 495-506.
16. W. Lei, V. N. Mochalin, D. Liu, S. Qin, Y. Gogotsi and Y. Chen, *Nat Commun*, 2015, **6**, 8849.
17. S. Chen, R. Xu, J. Liu, X. Zou, L. Qiu, F. Kang, B. Liu and H. M. Cheng, *Adv Mater*, 2019, **31**, e1804810.
18. C. Cao, Y. Xue, Z. Liu, Z. Zhou, J. Ji, Q. Song, Q. Hu, Y. Fang and C. Tang, *2D Materials*, 2019, **6**.
19. J. R. White, B. de Poumeyrol, J. M. Hale and R. Stephenson, *J. Mater. Science*, 2004, **39**, 3105-3114.
20. M. J. Ramsay and W. W. Clark, *Smart Structures and Materials 2001: Industrial and Commercial Applications of Smart Structures Technologies*, 2001, **4332**, 429 – 438.
21. Z. L. Wang, *Nano Res.*, 2008, **1**, 1-8.
22. Z. L. Wang, *Nano Today*, 2010, **5**, 512-514.
23. E. Fukada and I. Yasuda, *Japan. J. Appl. Phys.*, 1964, **3**, 117-121.
24. Y. Liu, H. L. Cai, M. Zelisko, Y. Wang, J. Sun, F. Yan, F. Ma, P. Wang, Q. N. Chen, H. Zheng, X. Meng, P. Sharma, Y. Zhang and J. Li, *Proc Natl Acad Sci U S A*, 2014, **111**, E2780-2786.
25. E. Fukada and I. Yasuda, *J. Phys. Soc. Japan*, 1957, **12**, 1158-1162.
26. E. Fukada, *J. Phys. Soc. Jap.*, 1955, **10**, 149-154.
27. B. Y. Lee, J. Zhang, C. Zueger, W. J. Chung, S. Y. Yoo, E. Wang, J. Meyer, R. Ramesh and S. W. Lee, *Nat. Nanotechnol.*, 2012, **7**, 351-356.
28. E. Fukada, *IEEE Transactions on Electrical Insulation*, 1992, **27**, 813-819.
29. G. Albrecht and R. B. Corey, *J. Am. Chem. Soc.*, 1939, **61**, 1087-1103.
30. Y. Iitaka, *Nature*, 1959, **183**, 390-391.
31. Y. Iitaka, *Acta Crystallographica*, 1958, **11**, 225-226.
32. A. Dawson, D. R. Allan, S. A. Belmonte, S. J. Clark, W. I. F. David, P. A. McGregor, S. Parsons, C. R. Pulham and L. Sawyer, *Cryst. Growth Des.*, 2005, **5**, 1415-1427.
33. R. Ashok Kumar, R. Ezhil Vizhi, N. Vijayan and D. Rajan Babu, *Physica B: Condensed Matter*, 2011, **406**, 2594-2600.
34. A. Heredia, V. Meunier, I. K. Bdikin, J. Gracio, N. Balke, S. Jesse, A. Tselev, P. K. Agarwal, B. G. Sumpter, S. V. Kalinin and A. L. Kholkin, *Adv. Funct. Mater.*, 2012, **22**, 2996-3003.
35. N. Balke, I. Bdikin, S. V. Kalinin and A. L. Kholkin, *J. Am. Ceramic Soc.*, 2009, **92**, 1629-1647.
36. V. J. González, A. M. Rodríguez, V. León, J. Frontiñán-Rubio, J. L. G. Fierro, M. Durán-Prado, A. B. Muñoz-García, M. Pavone and E. Vázquez, *Green Chemistry*, 2018, **20**, 3581-3592.
37. A. C. Ferrari, *Solid State Commun.*, 2007, **143**, 47-57.
38. A. C. Ferrari and D. M. Basko, *Nat. Nanotechnol.*, 2013, **8**, 235-246.
39. D. Fan, J. Feng, J. Liu, T. Gao, Z. Ye, M. Chen and X. Lv, *Ceramics International*, 2016, **42**, 7155-7163.
40. D. Lee, B. Lee, K. H. Park, H. J. Ryu, S. Jeon and S. H. Hong, *Nano Lett*, 2015, **15**, 1238-1244.
41. G. Liu and N. Komatsu, *ChemNanoMat*, 2016, **2**, 500-503.
42. A. Berkdemir, H. R. Gutiérrez, A. R. Botello-Méndez, N. Perea-López, A. L. Elías, C.-I. Chia, B. Wang, V. H. Crespi, F.

López-Urías, J.-C. Charlier, H. Terrones and M. Terrones, *Scientific Reports*, 2013, **3**.
43. R. Shahzad, T. Kim and S.-W. Kang, *Thin Solid Films*, 2017, **641**, 79-86.
44. L. Cao, S. Emami and K. Lafdi, *Materials Express*, 2014, **4**, 165-171.
45. R. B. Baig and R. S. Varma, *Chem. Soc. Rev.*, 2012, **41**, 1559-1584.
46. E. Er, H.-L. Hou, A. Criado, J. Langer, M. Möller, N. Erk, L. M. Liz-Marzán and M. Prato, *Chemistry of Materials*, 2019, **31**, 5725-5734.
47. X. Wang and P. Wu, *ACS Appl Mater Interfaces*, 2018, **10**, 2504-2514.
48. N. V. Surovtsev, S. V. Adichtchev, V. K. Malinovsky, A. G. Ogienko, V. A. Drebushchak, A. Y. Manakov, A. I. Ancharov, A. S. Yunoshev and E. V. Boldyreva, *J Chem Phys*, 2012, **137**, 065103.
49. Z. Liu, L. Zhong, P. Ying, Z. Feng and C. Li, *Biophys Chem*, 2008, **132**, 18-22.
50. A. M. Rodriguez, A. B. Munoz-Garcia, O. Crescenzi, E. Vazquez and M. Pavone, *Phys. Chem. Chem. Phys.*, 2016, **18**, 22203-22209.
51. S. Guerin, A. Stapleton, D. Chovan, R. Mouras, M. Gleeson, C. McKeown, M. R. Noor, C. Silien, F. M. F. Rhen, A. L. Kholkin, N. Liu, T. Soulimane, S. A. M. Tofail and D. Thompson, *Nat Mater*, 2018, **17**, 180-186.